Available online at www.sciencedirect.com
ScienceDirect
Journal of Sound and Vibration 302 (2007) 760–776
JOURNAL OF SOUND AND VIBRATION
www.elsevier.com/locate/jsvi

Influence of overpressure on sound transmission through curved panels

Bilong Liu*, Leping Feng, Anders Nilsson

MWL, Department of Aeronautical and Vehicle Engineering, KTH (The Royal Institute of Technology), Stockholm, SE-100 44, Sweden

Received 18 May 2005; received in revised form 4 December 2006; accepted 5 December 2006
Available online 23 February 2007

Abstract

A great deal of recent research related to the aeronautic industry has been devoted to the theoretical study of sound transmission through fuselage structures. However, the literature records few test data with reference to the influence of overpressure on sound transmission. In this article, the airborne sound transmission through curved panels under the condition of overpressure at the concave side has been investigated experimentally and it is shown that experimental results agree well with a theoretical prediction due to an infinite cylindrical shell model at relatively high frequencies. Discrepancies, which occur at lower frequencies, can be explained, *inter alia*, by the influence of the finite size and attached stiffeners of the panel.

At frequencies higher than the corresponding ring frequency for the curved panel, both experimental and theoretical predictions reveal that the overpressure at the concave side tends to reduce the sound transmission loss at the rate of about 0.5 dB/10 000 Pa. While at lower frequencies, say well below the ring frequency, the overpressure may increase or reduce sound transmission loss of a finite panel depending on the shift of resonant frequencies resulting from the overpressure.

1. Introduction

Infinite cylindrical shell theory is commonly used to model the sound transmission through fuselage structures [1–10]. Results show that there are two major dips in sound transmission loss of a larger diameter cylindrical shell. The first dip occurs at the cylinder ring frequency, where the interaction of bending forces and membrane forces in the shell leads to a minimum impedance for the structure. The second dip appears at the coincident frequency, where the wavenumber of the structural bending waves are equivalent to the acoustic waves. And when the frequency reaches twice that of the ring frequency, the shell behaves similarly to that of a flat panel.

Compared with curvature effects, the influence of internal pressurization has received little attention in the literature, see Refs. [2,3,11,12]. Generally speaking, internal pressurization results in three effects, viz. the out-of plane deformation of skins, an increase of in-plane membrane tensions, and the mismatch of the acoustic

*Corresponding author. Current address: The Institute of Acoustics, Chinese Academy of Sciences, 100080 Beijing, PR China. Tel.: +86 10 82610737; fax: +86 10 62553898.
E-mail address: liubl@mail.ioa.ac.cn (B. Liu).

0022-460X/$ - see front matter © 2007 Elsevier Ltd. All rights reserved.
doi:10.1016/j.jsv.2006.12.014

properties between internal and external fluid. The aircraft skins are usually attached to extremely stiff stringers and frames, which prevent any large out-of plane deformation of the panels from pressure difference at both sides. It is thus reasonable to assume that the resultant out-of plane deformation is negligible. The relation between the pressure difference and the in-plane tensions may then follow basic membrane theory. Hence, the effects of the overpressure on sound transmission loss can be evaluated by including the in-plane tensions within the dynamic model for the panel. Theoretical results based on infinite isotropic shell and plate models indicate that increasing in-plane tension results in kind of reduction of sound transmission loss, Refs. [3,11]. The mismatch of acoustics properties between internal and external medium can also be included in a theoretical model directly.

Although much research has been devoted to modelling the sound transmission through fuselage partitions, the literature records no test data relating to the influence of overpressure on sound transmission. Experimental work is an important and efficient procedure for investigating airborne sound insulation properties of panels, especially for those complicated structures such as large aircraft panels, for which theoretical modelling is not realisable. In this article, the airborne sound transmission through aircraft panels under the condition of overpressure at the concave side has been investigated by laboratory measurements. The test results are compared with the theoretical predictions based on the infinite cylindrical shell model according to Ref. [3] and the finite stiffening panel model developed in this article.

2. Experimental set-up and measurement

A description of the experimental set-up and measurement data for the influence of overpressure on the sound transmission loss is given in this section.

2.1. Test set-up and panel description

The sound transmission loss is measured according to standard ISO 15186-1:2000 [13] with intensity method (Fig. 1). The test sample is mounted in between a reverberation room and an anechoic room. The reverberation room 6.21 m × 7.86 m × 5.05 m is treated as a source room and a rotating microphone is used to measure average sound pressure level. The anechoic room (7 m × 5.95 m × 5.8 m, cut-off frequency 80 Hz) is utilized as a receiving room and the average sound intensity level over the sample surface is measured by the scanning method. The procedure of measurement is in full accordance with the standard mentioned above. The laboratory facilities available to the authors at Marcus Wallenberg Laboratory for Sound and Vibration Research (MWL), KTH, Sweden are well equipped for sound transmission loss experiments giving repeatability for measurements less than 0.5 dB throughout the given frequency range. In addition, the anechoic room at MWL can be pressurized, with a maximum overpressure of 8500 Pa, to gauge the influence of the overpressure on sound reduction index. The intensity sound reduction index (or sound transmission

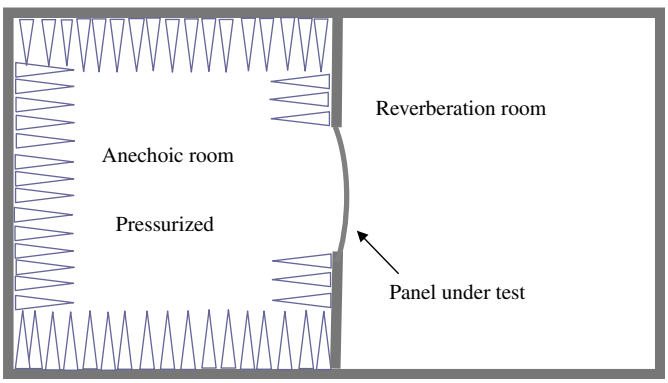

Fig. 1. Set-up for transmission loss (TL) measurements.

loss) is calculated according to the standard as

$$\mathrm{TL}_I = L_{pi} - 6 - (L_{\mathrm{In}} + 10\log(S_m/S)), \tag{1}$$

where L_{pi} is the averaged sound pressure level in the source room and L_{In} is the averaged sound intensity level over the panel surface measured in the anechoic room, S_m is the measurement area and S is the area of the test specimen. For the measurements examined in this article, $S_m = S$.

When the anechoic room is pressurized, the air density inside the anechoic room is increased to $\rho_{\Delta P}$, with the relation to ρ_0 as

$$\rho_{\Delta P} = \frac{\Delta P + P_{\mathrm{atm}}}{P_{\mathrm{atm}}}\,\rho_0, \tag{2}$$

where ρ_0 air density without overpressure, ΔP is the overpressure, P_{atm} is ambient atmosphere pressure.

Three panels shown in Table 1 were measured to assess the overpressure effects. In Table 1, Panel A and B are large aircraft panels (same as Panel G and Panel H in Ref. [14], respectively). Panel C is an aluminium panel with two steel ribs attached (same as Panel D in Ref. [14]). Panel A is a metallic panel and B is a composite panel with the same weight and a similar structural arrangement. Panels A and B were stiffened with stringers and ring frames and heavily damped at the concave side. The stringers cover around 60% of the panel; the remaining part without the stringer is designed for allocation of windows. Therefore, two areas, the stringer and window area, may be classified for Panels A and B. It must be noted that the panel thickness for the stringer area and window area are not the same. To avoid the complexity in a prediction model, the equivalent thicknesses, for example 2.0 mm for Panel A and 3.3 mm for Panel B, were adopted in the calculations. In the experiment the panels were clamped at the boundaries. Also, it is important to note that the ring ribs for Panel C are wide, extremely heavy and stiff in comparison with the skin panel.

2.2. Effects of overpressure on sound transmission loss

Values for sound transmission losses from Panel A, measured with and without overpressure, are shown in Fig. 2. For convenience of exposition the influence of the overpressure, Fig. 3 shows the difference of sound transmission losses with step-up overpressure. The data obtained for different overpressures are consistent, indicating the reliability of the measurements.

For Panel A, it is evident in Fig. 2 that two frequency ranges can be classified to describe the overpressure effects. In the frequency range above 160 Hz, the overpressure reduces the sound transmission loss of the panel. It was found that the TL reduction was less than 1 dB in this frequency range for overpressures up to 8500 Pa. Below 160 Hz, however, the overpressure seems to increase the sound transmission loss by a few decibels.

The tendency for the overpressure to reduce sound transmission loss at relatively high frequencies can be predicted by an infinite shell model by including the increase of in-plane tension. Whilst the increase of sound transmission loss at lower frequencies may be caused by the shift of resonances due to the combined influence of increasing in-panel tension and the finite-size of the panel, see the prediction model in Section 3.

Sound transmission losses for Panel B, measured with and without overpressure, are shown in Figs. 4 and 5. On comparison of Figs. 4 and 5 with Figs. 2 and 3, it may be concluded that the overpressure influence on the metallic and composite panels is roughly the same, indicating that the overpressure effects are not sensitive to the panel material.

Table 1
Panels used in measurement

Panel	Material	Radius (m)	Size (m^2)	Density of skin (kg/m^2)	Young's modulus (N/m^2)	Loss factor
A	Metallic	2	1.67×2.2	5.4	6.85×10^{10}	Ref. [14]
B	Composite	2	1.67×2.2	5.4	3.25×10^{10}	
C	Aluminum	1	0.87×0.95	2.7	6.85×10^{10}	0.01

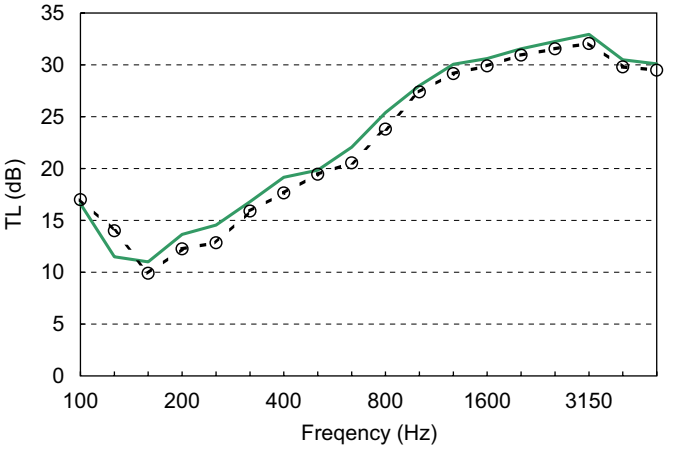

Fig. 2. Comparison of measured TL, with and without overpressure at the anechoic room side: —— 0 Pa; ---○--- 8500 Pa; Panel A, $f_R = 420$ Hz.

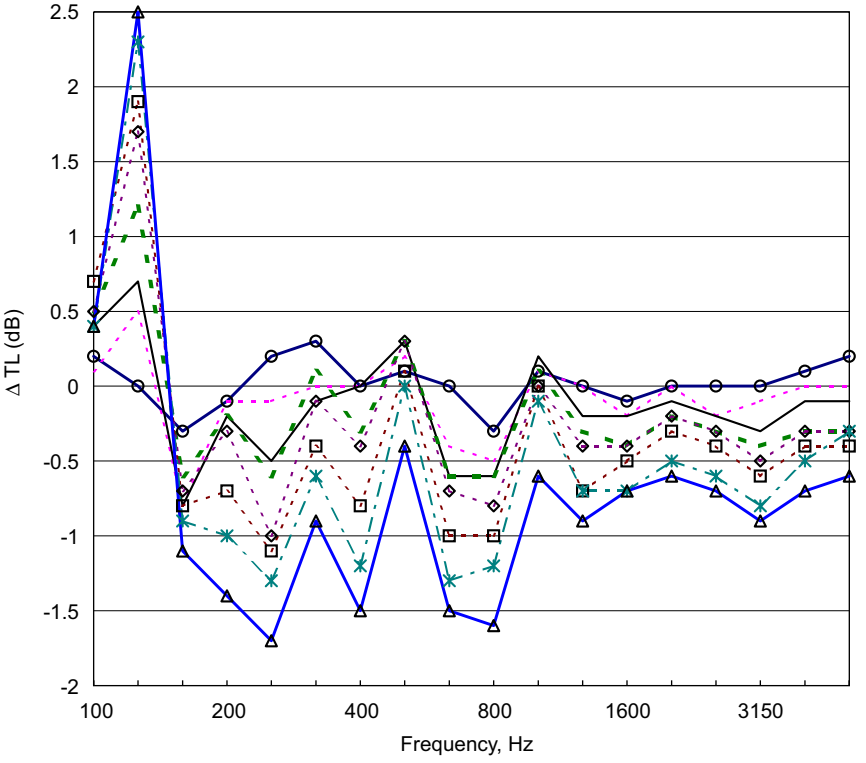

Fig. 3. Measured TL difference with step-up overpressure: —○— 1000 Pa; -----2000 Pa; —— 3000 Pa; ▬▬▬ 4000 Pa; ---◇--- 5000 Pa; ---□--- 6000 Pa; ---*--- 7500 Pa; _△_ 8500 Pa; Panel A, $\Delta TL = TL_{\text{with pressure difference}} - TL_{\text{without pressure difference}}$.

Sound transmission losses of a relatively smaller aluminium panel, measured with and without overpressure, are shown in Figs. 6 and 7. Two frequency ranges may be classified to describe the overpressure influence on sound transmission loss. When the overpressure at concave side of panel is increased up to 5000 Pa, it is found that the sound transmission loss decreases by 0.5 dB above the corresponding ring frequency for Panel C. Below the ring frequency, it seems that the overpressure may increase or decrease the sound transmission loss, depending on the frequency range observed. The variation of sound transmission loss up to 2.0 dB is observed

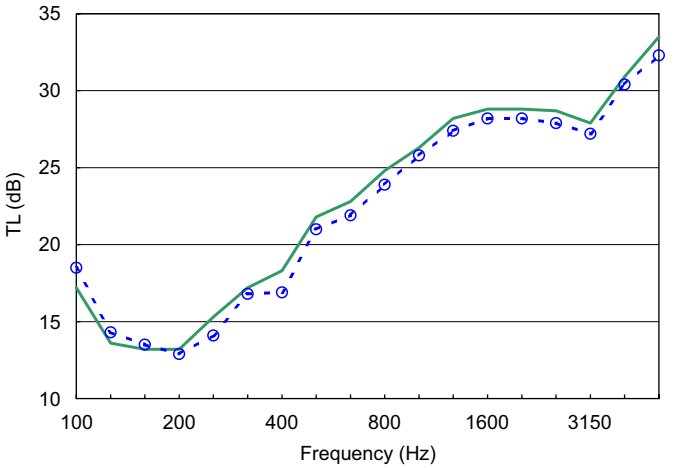

Fig. 4. Comparison of measured TL, with and without overpressure at the anechoic room side: —— 0 Pa; ---○--- 8500 Pa; Panel B, $f_R = 370$ Hz.

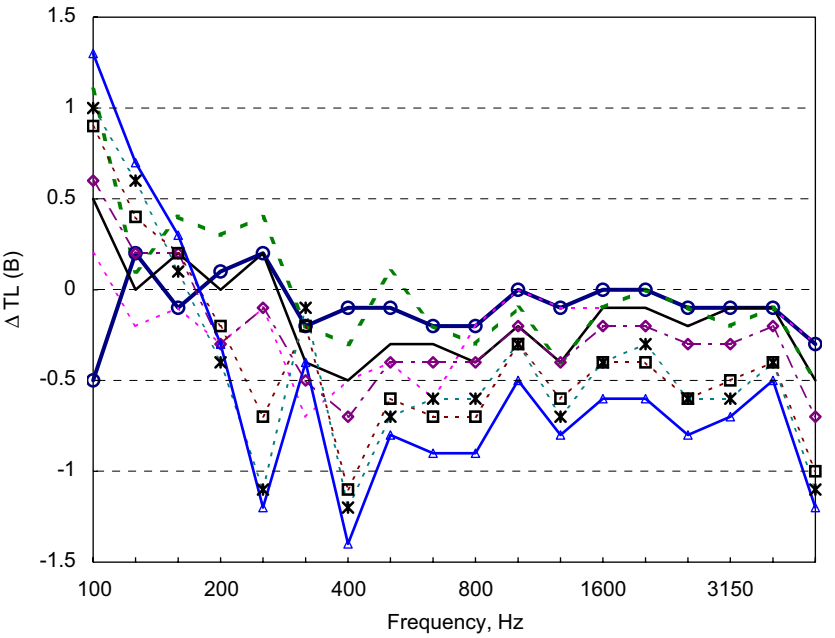

Fig. 5. Measured TL difference with step-up overpressure: —○— 1000 Pa; -----2000 Pa; —— 3000 Pa; ▬▬▬ 4000 Pa; ---◇--- 5000 Pa; ---□--- 6000 Pa; ---*--- 7500 Pa; —△— 8500 Pa; Panel B, $\Delta TL = TL_{\text{with pressure difference}} - TL_{\text{without pressure difference}}$.

for the measurement. If now comparing Panel C with Panels A and B, it may be observed that the overpressure effects on sound insulation at lower frequencies are not similar, indicating that the overpressure effects on sound transmission loss at the lower frequencies are sensitive to the finite size of the panel.

3. Theoretical prediction and models

Theoretical models in describing the curved panel configuration are developed in this section. The section begins with a description of the infinite cylindrical shell model.

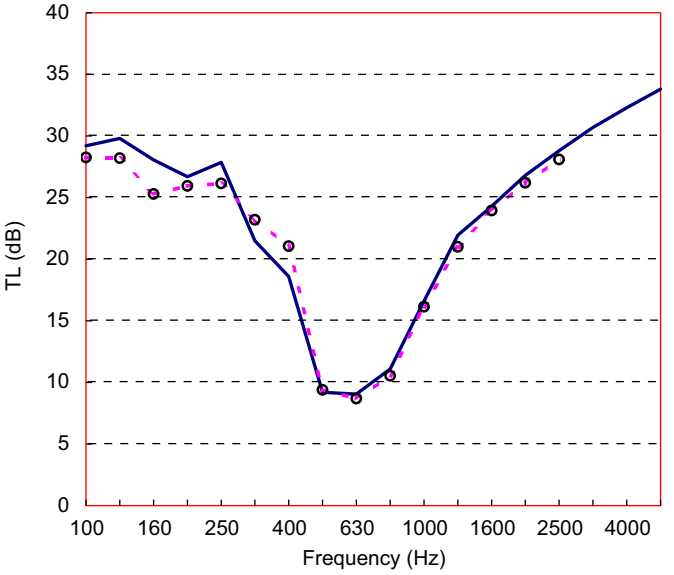

Fig. 6. Comparison of measured TL, with and without overpressure at the anechoic room side: —— 0 Pa; ---○--- 5000 Pa; Panel C, $f_R \approx 850$ Hz.

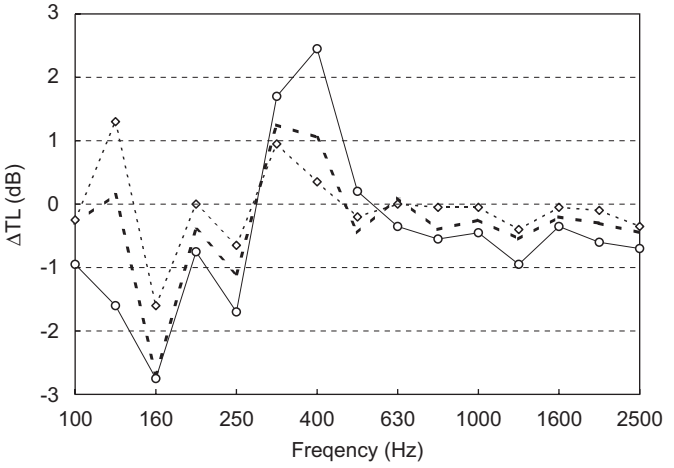

Fig. 7. Measured TL difference with step-up overpressure: ---◇--- 2000 Pa; -----3000 Pa; —○— 5000 Pa; $\Delta TL = TL_{\text{with pressure difference}} - TL_{\text{without pressure difference}}$, Panel C.

3.1. Model of infinite curved panel

Before considering the problem of sound transmission through a pressurized fuselage panel, a brief review of the basic formulae for sound transmission through an infinite flat panel (see Fig. 8) is given. The field incident transmission loss of the infinite flat panel is defined by Eq. (3), see Refs. [3]

$$TL = -10 \log \bar{\tau}, \tag{3}$$

where

$$\bar{\tau} = \frac{\int_{\beta=0}^{2\pi} \int_{\theta=0}^{78^\circ} \tau(\theta_1, \varphi) \sin \theta_1 \cos \theta_1 d\theta_1 d\varphi}{\int_{\beta=0}^{2\pi} \int_{\theta=0}^{78^\circ} \sin \theta_1 \cos \theta_1 d\theta_1 \, d\varphi}, \tag{4}$$

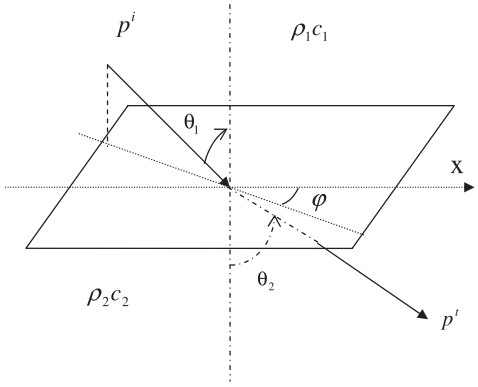

Fig. 8. Schema of sound transmission through an infinite flat panel.

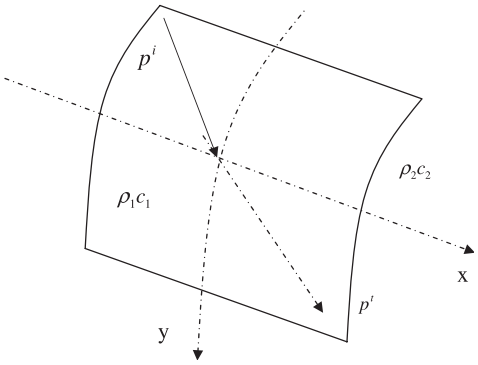

Fig. 9. Geometry of cylindrical panel.

$$\tau(\theta_1,\varphi)=\frac{4\rho_1 c_1}{\rho_2 c_2}\left|\left[1+\frac{\rho_1 c_1}{\rho_2 c_2}\frac{\cos\,\theta_2}{\cos\,\theta_1(1+M\,\cos\,\varphi\sin\,\theta_1)}\right]+\frac{Z_p}{\rho_2 c_2}\cos\,\theta_2\right|^{-2}, \tag{5}$$

$$\sin\,\theta_2=(c_2/c_1)\sin\,\theta_1(1+M\,\cos\,\varphi\,\sin\,\theta_1)^{-1}, \tag{6}$$

M is Mach number of the airflow; Z_p refers to impedance of the infinite flat panel. The symbol $\bar{\tau}$ is the average of transmission efficiency, $\tau(\theta_1,\varphi)$ computed over the "truncated" hemisphere $78^\circ<\theta_1<0^\circ$, $0^\circ<\varphi<360^\circ$, θ_1 and φ are the angle of incident wave relative to the coordinate axes (Fig. 8), θ_2 and φ are the angles of the transmitted wave. The acoustic media have properties ρ_1, c_1 and ρ_2, c_2, for regions 1 and 2, respectively.

For a slightly curved panel with single side pressurization (Fig. 9) one may neglect the effect of wave diffraction resulting from curvature, Ref. [15], and substitute the shell panel impedance Z_s for Z_p in Eq. (5) to evaluate sound transmission loss. One example of the cylindrical panel impedance under condition of overpressure at one side is given in Ref. [3]

$$Z_s=\mathrm{i}m\omega\left[1-\frac{f^2}{f_{c2}^2}\cos^4\theta_2-\frac{f_R^2}{f^2}\cos^4\varphi-\frac{\cos^2\theta_2}{m_p c^2}\times(N_x\cos^2\varphi+N_y\sin^2\varphi)\right], \tag{7}$$

where $f_{c2}=(c_2^2/2\pi)\sqrt{m_p/D}$ is the coincident frequency of the panel, $f_R=(1/2\pi r)\sqrt{Eh/(m_p(1-\nu^2))}$ is the ring frequency for an equivalent full cylinder of radius r, D the bending stiffness, E the Young's modulus. N_x, N_y are internal membrane stresses resulting from pressurization. If the aircraft fuselage is modelled as a cylinder

with two end plates then the membrane stresses N_x, N_y can be assumed to take the approximate values (see Ref. [3])

$$N_x = \Delta PR/2, \quad N_y = \Delta PR. \tag{8}$$

3.2. Calculation of pressurization effects for infinite curved panel

For a general enclosed structure an internal atmospheric pressurization results in the increase of in-plane membrane tensions and a mismatch of internal–external acoustic properties. It is therefore of interest to see how these factors affect sound transmission loss. In order to observe the effects step by step, the influences of in-plane membrane tensions and the mismatch of acoustic properties are evaluated separately. Later the overall influence is discussed. The comparison between measurement and prediction based on the infinite model will be presented. The panel parameters used in calculation are shown in Table 2.

3.2.1. Influence of in-plane membrane tensions resulting from overpressure

Examples of the influence of in-plane membrane tensions, resulting from overpressure, on sound transmission loss are shown in Fig. 10. For convenience of exposition, Fig. 11 shows the difference of sound transmission loss when there is overpressure and when there is no overpressure.

Two dips, corresponding to ring frequency and coincident frequency, can be found in Fig. 10. At the ring frequency, the interaction of membrane and bending forces in a shell results in theoretical zero impedance value for the shell. While at the coincident frequency, the panel structural wavenumber is the same as the acoustic wavenumber, which leads to a minimum impedance for the panel. Between ring frequency and coincident frequency, the in-plane membrane tension reduces sound transmission loss with the rate of about 0.25 dB/0.1 atm. Below ring frequency the curvature of the panel increases its stiffness forcing the structure to become less sensitive to the in-plane tension. The sound transmission loss is reduced at the rate around 0.08 dB/0.1 atm. Also it may be noted that the appearance of in-plane tension causes a small decrease in the

Table 2
Panel parameters used in calculation

Panel	Material	Area density (kg/m^2)	Radius (m)	Young's modulus (N/m^2)	Poisson ratio	Loss factor
D	Aluminum	4.05	2	6.85E+10	0.3	0.01

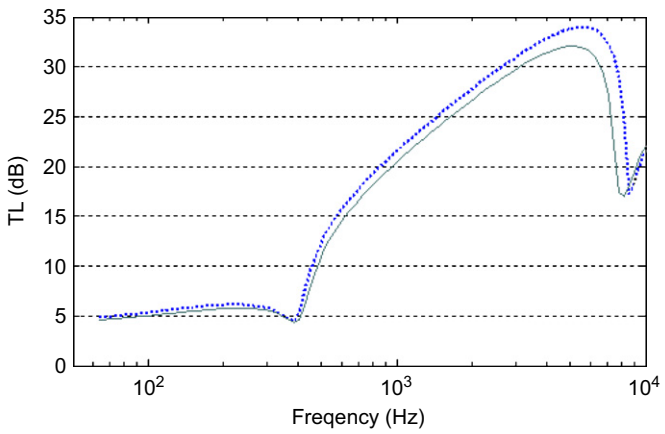

Fig. 10. Predicted TL when there is in-plane tension difference, ------ $\Delta P = 0$ atm; —— $\Delta P = 0.5$ atm; Panel D.

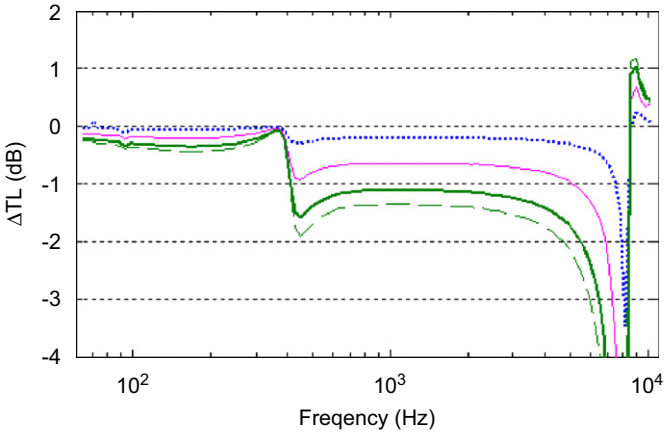

Fig. 11. Predicted TL difference when there is in-plane tension difference: ▬▬▬ $\Delta P = 0.1$ atm; —— $\Delta P = 0.3$ atm; ▬▬▬ $\Delta P = 0.5$atm; - - - - - - - $\Delta P = 0.6$ atm; $\Delta TL = TL_{\text{with in-plane tension difference}} - TL_{\text{without in-plane tension difference}}$, Panel D.

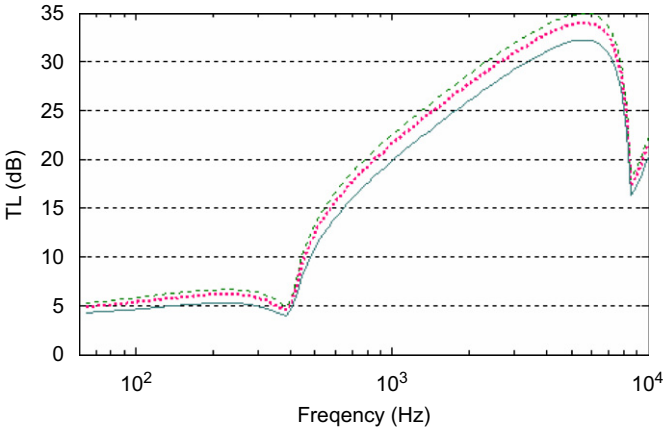

Fig. 12. Predicted TL when there is mismatch of air density: - - - - - - $\gamma_1 = 0.8$; ▬▬▬ $\gamma_1 = 1.0$; —— $\gamma_1 = 1.5$; Panel D.

coincident frequency. This gives an explanation of the large *jump* in the difference of the sound transmission loss around the coincident frequency (Fig. 11).

3.2.2. *Influence of mismatch of acoustic properties on sound transmission loss*

The overpressure introduces a mismatch of acoustic properties between external and internal fluid. To assess the influence of mismatch of acoustic properties several limiting cases are considered in calculation.

(1) Both sides have same sound speed but different air density. The measurement performed at MWL laboratory is similar to this situation, where the overpressure results in mismatch of air density between the pressurized room (Anechoic Room) and no pressurized room (Reverberant Room), while the sound speeds are roughly the same. Eq. (5), in this case, may be rewritten as

$$\tau(\theta_1, \beta) = \frac{4}{\gamma_1}\left(1 + \frac{1}{\gamma_1} + \frac{Z_p}{\gamma_1 \rho_1 c_1}\cos\,\theta_1\right)^{-2} \tag{9}$$

with the ratio $\gamma_1 = \rho_2/\rho_1$. Using Eq. (9), the influence of mismatch of air density resulting from overpressure on sound transmission loss may be evaluated.

Fig. 12 presents examples of the dependence of sound transmission loss on the mismatch of air density. In the following calculations, the reference fluid properties are assumed to be in ambient room conditions, i.e.,

$\rho_1 = 1.21\,\mathrm{kg/m^3}$ and $c_1 = 340\,\mathrm{m/s}$. Therefore a value $\gamma_1 > 1$ indicates there is an overpressure at one side, and $\gamma_1 < 1$ indicates an under pressure. Calculations show that increasing the ratio γ_1 results in a decrease of sound transmission loss over the entire frequency range. A 10% increase in γ_1 results in about 0.4 dB reduction of sound transmission loss between the ring frequency and the coincident frequency, and about 0.2 dB below the ring frequency. Except near coincident frequencies, the calculation shows that influence of the mismatch of air density on the sound transmission loss is larger than that of variation of in-plane membrane tension led by an overpressure.

(2) Both sides, left and right, have the same air density but different sound speed. In this case, Eq. (3) can be rewritten as

$$\tau(\theta_1, \beta) = \frac{4}{\gamma_2}\left(1 + \frac{1}{\gamma_2}\frac{\sqrt{1-\gamma_2^2\sin^2\theta_1}}{\cos\,\theta_1} + \frac{Z_p}{\gamma_2\rho_1 c_1}\sqrt{1-\gamma_2^2\sin^2\theta_1}\right)^{-2}, \tag{10}$$

where $\gamma_2 = c_2/c_1$. This case is not commonly seen in practice. However, it is still of interest to evaluate the influence of the mismatch of sound speed on sound transmission loss.

Examples of the variation of sound transmission loss resulting from mismatch of sound speed at two sides of the panel are shown in Fig. 13. Again, the reference fluid properties used in calculation are assumed $\rho_1 = 1.21\,\mathrm{kg/m^3}$ and $c_1 = 340\,\mathrm{m/s}$. Similar to the air density mismatch study, the sound transmission loss decreases when the ratio γ_2 is greater than unity. For the case studied, a 10% increase in γ_2 results in the reduction of sound transmission loss around 2.5 dB between the ring frequency and the coincident frequency, and about 0.8 dB below the ring frequency. It is interesting to note that sound transmission loss for sound speed mismatch is more sensitive in comparison with air density mismatch. This reason is that the mismatch of sound speed results in not only a direct acoustic impedance mismatch $\rho_2 c_2/\rho_1 c_1$, but also in wave refraction, within various expressions in expression Eq. (10).

(3) Comparison of overpressure influence between ambient *ground* condition ($\rho_2 = \rho_1 = 1.21\,\mathrm{kg/m^3}$, $c_2 = c_1 = 340\,\mathrm{m/s}$, $\Delta P = 0\,\mathrm{Pa}$) and *cruising flight* condition at 10660 m with fuselage interior pressurized to 2440 m ($\rho_1 = 0.382\,\mathrm{kg/m^3}$, $c_1 = 299\,\mathrm{m/s}$, $\rho_2 = 0.967\,\mathrm{kg/m^3}$, $c_2 = 340\,\mathrm{m/s}$, $\Delta P = 50\,000\,\mathrm{Pa}$). Since the influence of overpressure is of specific interest in this paper, the Mach number is set to zero in the calculation for flight conditions.

Without taking into account the speed of air flow ($M = 0$), Fig. 14 shows the in-plane tension, resulting from pressurization, reducing sound transmission loss about 1.25 dB between ring and coincident frequency, and about 0.4 dB below ring frequency. The mismatch of acoustic properties improves sound transmission by about 4.0–5.0 dB throughout the whole frequency range. The total influence on sound transmission loss resulting from mismatch of acoustics properties and in-plane tension is around 3.0–4.0 dB.

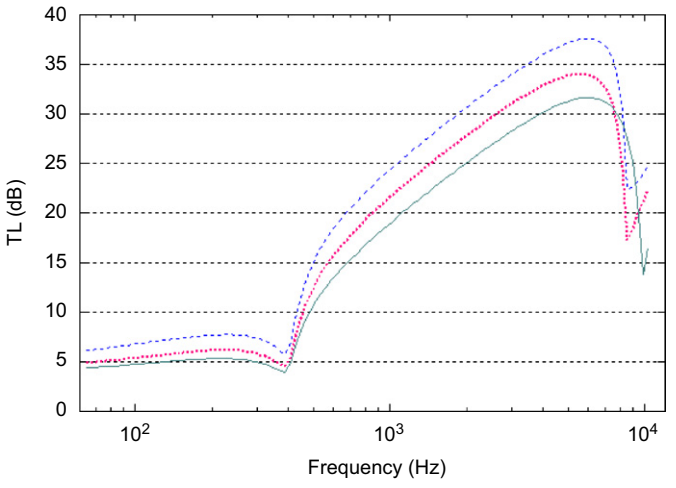

Fig. 13. Influence of mismatch of sound speed on TL: ------ $\gamma_2 = 0.9$; ▬▬▬▬ $\gamma_2 = 1.0$; —— $\gamma_2 = 1.1$; Panel D.

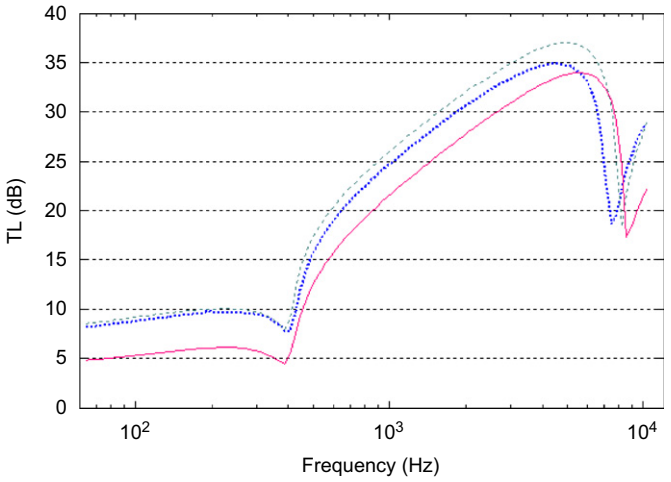

Fig. 14. TL between ground condition and cruising flight height ($M = 0$): ------ $\rho_1 = 0.382\,\mathrm{kg/m^3}$, $\rho_2 = 0.967\,\mathrm{kg/m^3}$, $c_1 = 299\,\mathrm{m/s}$, $c_2 = 340\,\mathrm{m/s}$, $\Delta P = 0\,\mathrm{atm}$; ▬▬▬ $\rho_1 = 0.382\,\mathrm{kg/m^3}$, $\rho_2 = 0.967\,\mathrm{kg/m^3}$, $c_1 = 299\,\mathrm{m/s}$, $c_2 = 340\,\mathrm{m/s}$, $\Delta P = 0.5\,\mathrm{atm}$; —— $\rho_1 = \rho_2 = 1.21\,\mathrm{kg/m^3}$, $c_1 = c_2 = 340\,\mathrm{m/s}$, $\Delta P = 0\,\mathrm{atm}$; Panel D.

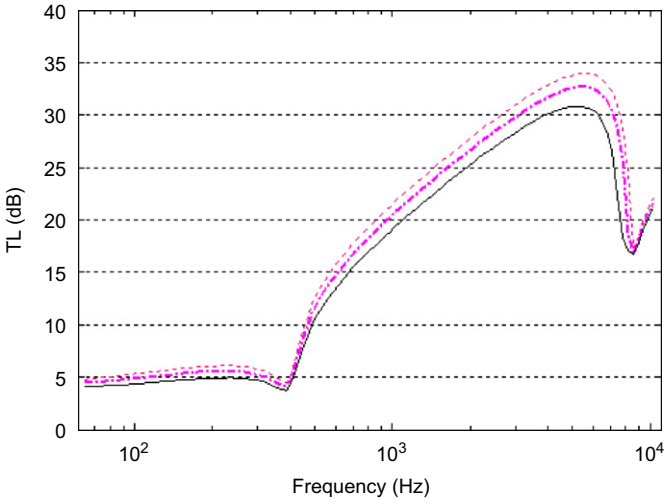

Fig. 15. Predicted overpressure influence on TL, laboratory condition: ------ $\Delta P = 0\,\mathrm{atm}$; ▬▬▬ $\Delta P = 0.2\,\mathrm{atm}$; —— $\Delta P = 0.5\,\mathrm{atm}$; Panel D.

The final example in this section shows the influence of overpressure on sound transmission loss for the same panel in laboratory conditions. For real aircraft structures, skin panels are usually attached with stringers in the axial direction. The stringers are extremely stiff and densely arranged and undertake most of the in-plane tension due to overpressure in the axial direction. Therefore, for real aircraft skin panels, it is reasonable to assume that overpressure only results with in-plane tension in the circumferential direction, whilst the effect in the axial direction may be neglected. In this case, the relation of in-plane membrane tension and overpressure assumed by Eq. (8) may modified by

$$N_x = 0, \quad N_y = \Delta P \times R. \tag{11}$$

Eq. (11) is used to evaluate the influence of overpressure in laboratory conditions.

Results of influence of overpressure under laboratory conditions are shown in Fig. 15. At first glance it seems there is a contradiction between Figs. 14 and 15. Fig. 14 shows that the sound insulation properties at the flight condition are better than the ground condition, while Fig. 15 indicates that the pressure difference tends to reduce sound transmission loss in the laboratory condition. The reason for this "apparent" contradiction is the reference data: the ground condition is the reference state for both calculations. In the laboratory condition, the ground condition is also the condition of the room without overpressure (reverberation room). However, in the flight condition, the air density and sound speed outside the fuselage are much lower than that in the ground condition. Results shown in Fig. 14 are actually the effects of all influences, i.e. the lower air density, lower sound speed and the pressurization. Since the measurements are performed at ground level, it is quite reasonable to gather and infer some knowledge of the difference of overpressure influence between laboratory and practical flight conditions.

Under laboratory conditions, Fig. 15 shows that the overpressure at the concave side reduces sound transmission loss with a rate of about 0.5 dB/0.1 atm between ring frequency and coincident frequency, and about 0.2 dB/0.1 atm below ring frequency.

3.2.3. *Comparison between measurement and prediction*

Examples of the comparison between measurement and calculation based on the infinite model are shown in Fig. 16(a) and (b), corresponding to Panel A and B, respectively. In the calculation, the panels are modelled by curved, uniform panels with equivalent thickness, i.e., 2 mm for Panel A and 3.3 mm for Panel B.

It is evident that agreement between measurement and prediction is good at relatively high frequencies. At lower frequencies, however, the measurement and prediction results are less in agreement: the theoretical model predicts a decrease of sound transmission loss for all frequencies, while the measurements show an increase in sound transmission loss at low frequency. This indicates that the infinite model is not able to predict the acoustic performance of the finite stiffening panel at low frequencies, even if the change in sound transmission loss is of concern.

In order to overcome the discrepancies between measurement data and calculation results, one may improve the prediction model by considering a finite model with circumferential frame attachments. An analytical model based on modal expansion is developed in Ref. [14] to predict sound transmission loss for finite curved panels with and without circumferential frame attachments, the predicted overpressure influence on sound transmission loss, however, is given in the following section:

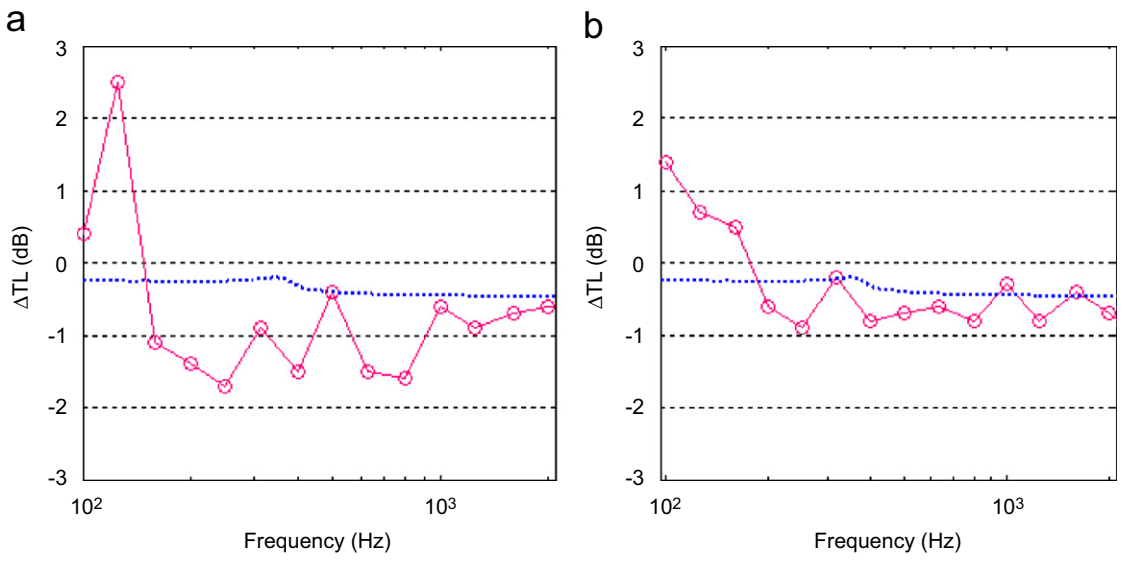

Fig. 16. Predicted overpressure influence on TL, comparison of measurement and prediction: —○— measurement; ------ predicted by infinite model; (a) Panel A; (b) Panel B; $\Delta P = 8500$ Pa, $\Delta TL = TL_{\text{with overpressure}} - TL_{\text{without overpressure}}$.

3.3. Calculation of overpressure effects for curved panels with ring stiffeners

3.3.1. Overpressure effects for curved panels

A 1 mm isotropic aluminium panel 0.87 m × 0.95 m, effective radius 1 m with a loss factor 0.01 is examined for sound transmission loss numerically. The laboratory conditions, viz., Eq. (2) and (11), are assumed in the calculations to investigate the mismatch of the acoustic properties and the in-plane tensions caused by the overpressure.

The influence of overpressure on sound transmission loss is shown in Fig. 17. For high frequencies, above twice that of the ring frequency, the influence of the overpressure is roughly the same as that for an infinite panel, i.e. the sound transmission loss decreases at the rate of about 0.5 dB /10 000 Pa.

If the frequency decreases further, the behaviour of the finite panel is somewhat different from that of an infinite panel. With overpressure, it is clear in Fig. 17 that the sound transmission loss up to 200 Hz is improved significantly, but as frequency increases the sound transmission loss is decreased. Experiments also support this observation: when the frequency is much lower than the corresponding ring frequency, the overpressure will increase the sound transmission loss rather than to decrease as for an infinite cylindrical shell. Unfortunately, experiments for this panel cannot reach this high level of overpressure due to safety reasons and hence are not shown in this diagram.

The reason for this phenomenon can be explained by the shift of the resonant frequencies of the panel due to the increase of the in-plane tension driven by the overpressure. It is not difficult to show that when the in-plane tension is increased and the panel becomes stiffer, all modes shift to higher frequencies, with the modes of high circumferential order shifting more since these modes are more membrane tension controlled. It is this shift of the resonant frequency that changes the performance of a finite, curved panel and sets it distinctly apart from an infinite cylindrical shell.

Fig. 18 shows the influence of the overpressure on the sound transmission loss of individual modes of the panel. The resonant frequency of each mode is located approximately at the frequency with the minimum sound transmission loss. When there is no overpressure, due to the curvature effect, the resonant frequency of the mode (1, 1) for this curved panel is about 400 Hz, and the resonant frequencies of the higher-order circumferential modes are located below 400 Hz, while the higher-order axial modes are higher than the first mode. When there is overpressure, the higher-order circumferential modes are shifted to higher frequencies, while axial modes are less affected. As a result, more modes are concentrated in the frequency region around half of the ring frequency ($f_R \approx 850$ Hz), and the sound transmission losses at the frequency bands nearby are

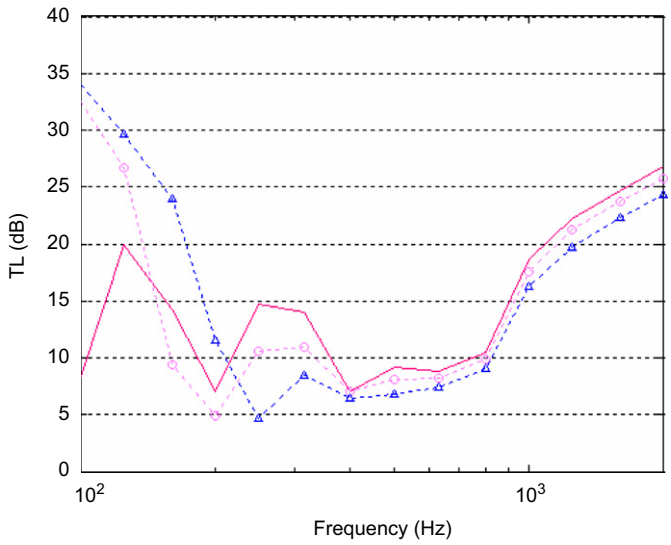

Fig. 17. Predicted overpressure influence on TL, 1mm aluminium panel: —— ΔP = 0 atm; - - -○- - - ΔP = 0.2 atm; - - -△- - - ΔP = 0.5 atm.

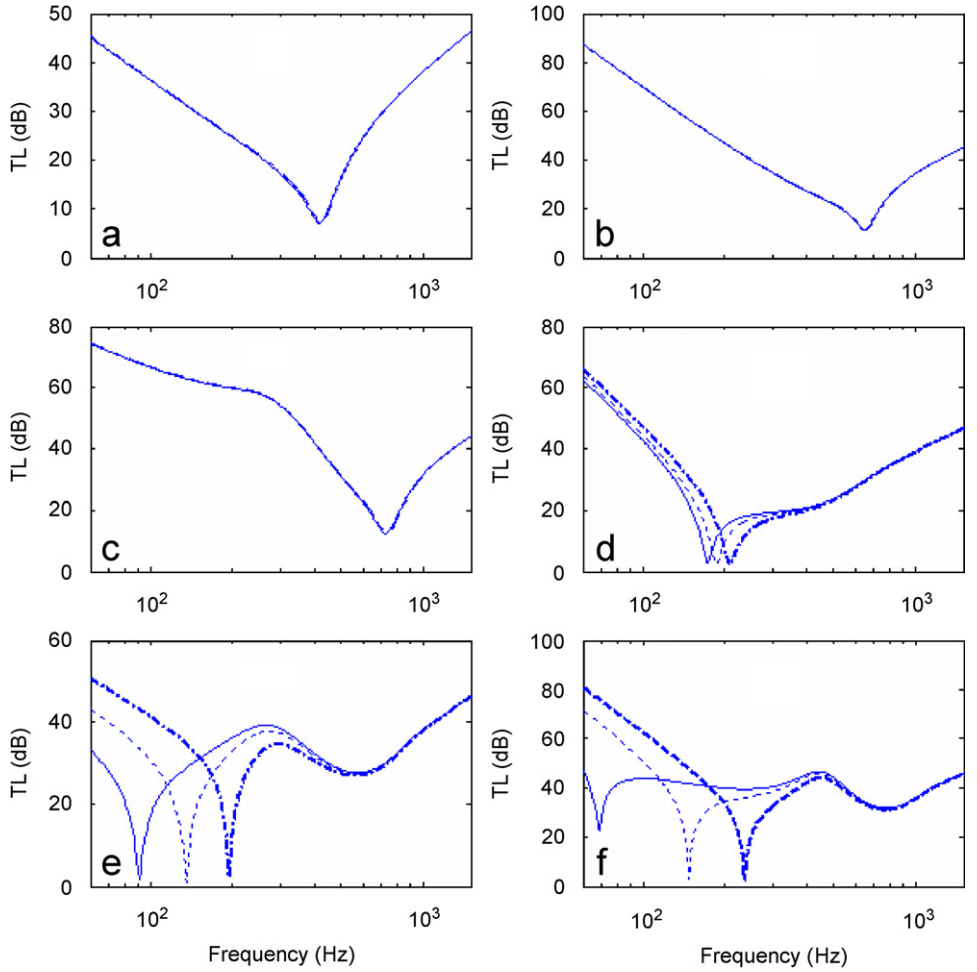

Fig. 18. Predicted overpressure influence on TL of individual modes, 1 mm aluminium panel: —— $\Delta P = 0$ atm; ------- $\Delta P = 0.1$ atm; ▬▬▬ $\Delta P = 0.3$ atm; (a) mode (1,1); (b) mode (2,1); (c) mode (3,1); (d) mode (1,2); (e) mode (1,3); (f) mode (1,4).

considerably reduced by the overpressure. In addition the sound transmission losses at lower frequency bands are increased by the overpressure, as fewer radiation-efficient modes exist.

3.3.2. *Overpressure effects for curved panels with ring stiffeners*

A panel with the same parameters as used in Section 3.3.1 but attached with two ring stiffeners is examined. The stiffener is assumed to be made of aluminium and equally spaced and has a rectangular cross-section with height 80 mm and width 2 mm. The loss factor 0.01 for the stiffener is assumed.

The acoustic behaviour of the panel with ring stiffeners, Figs. 19 and 20, with and without overpressure is similar to that of isotropic panel for relatively high frequencies. But at low frequencies, less fluctuation of sound transmission loss is observed for the ring-stiffened panel in comparison with that of the isotropic panels.

3.3.3. *Comparison of measurement and prediction*

Figs. 21 and 22 show the comparison between measurements and prediction for Panels A, B. As a reference, calculations based on infinite panel theory are also included in the figures. In a relatively high frequency range, for the studied case above ring frequency, the finite model including ring stiffeners and infinite isotropic model gives almost identical results of the overpressure influence. Results also agree well with measurements in the higher frequency range. At lower frequencies, the infinite model prediction significantly differs with the

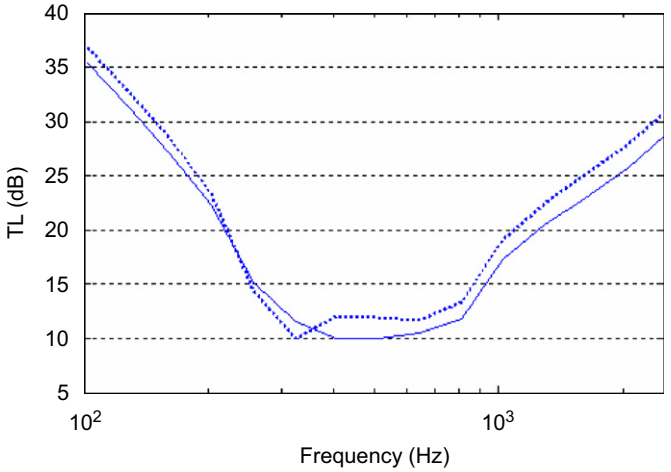

Fig. 19. Influence of overpressure on TL, 1 mm aluminium panel attached with two ring stiffeners, simply supported: ------ $\Delta P = 0.1$ atm; —— $\Delta P = 0.5$ atm.

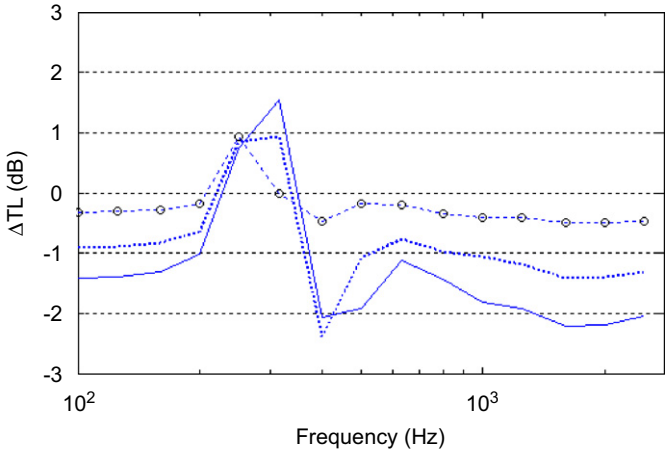

Fig. 20. Predicted overpressure influence on TL difference, 1 mm aluminium panel attached with two ring stiffeners, simply supported: ---○--- 0.1atm; ------ $\Delta P = 0.3$ atm; —— $\Delta P = 0.5$ atm.

measurements, while the finite model can still describe the performance of the panel correctly. Both panels experience some improvement of sound transmission loss caused by overpressure at low frequencies.

4. Concluding remarks

The airborne sound transmission through curved, aircraft panels under the influence of overpressure at the concave side has been investigated in this paper. The measurement data has been collated under laboratory conditions, and the theoretical model including finite size panels and ring stiffeners has been developed. It was found that the test results agree well with the theoretical prediction of infinite cylindrical shell model above the ring frequency, but considerable discrepancies occur well below the ring frequency. This has been explained partly through some assumptions within the theoretical model including a finite size panel and modelling of stiffeners of the panel.

At frequencies higher than the ring frequency, both test and theoretical results reveal that the overpressure under laboratory conditions tends to reduce the sound transmission loss at the rate of about 0.5 dB /10 000 Pa,

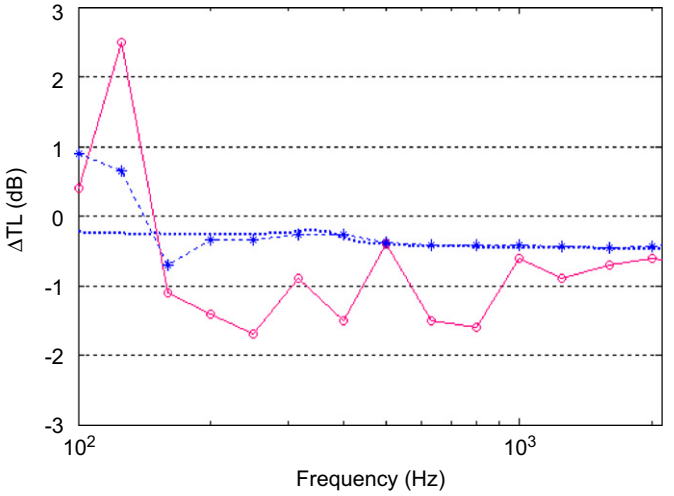

Fig. 21. Influence of overpressure on TL, comparison of measurement and prediction, $\Delta P = 8500\,\text{Pa}$, Panel A: —○— measurement; ------ predicted by infinite model; ---*--- predicted by finite model with stringer attachments, Ref. [14].

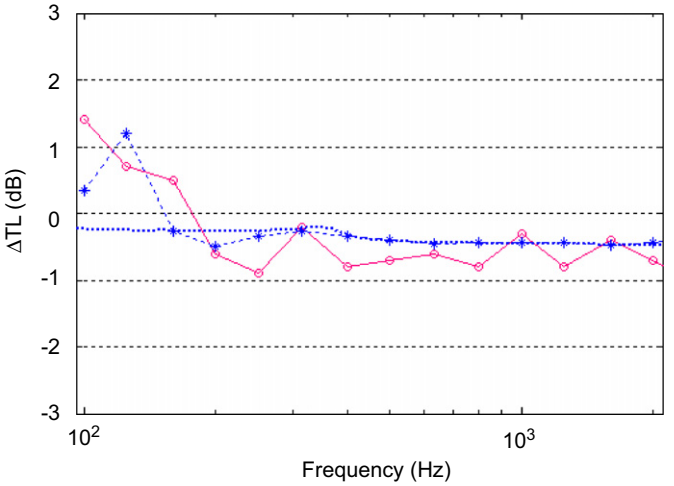

Fig. 22. Influence of overpressure on TL, comparison of measurement and prediction, $\Delta P = 8500\,\text{Pa}$, Panel B: —○— measurement; ------ predicted by infinite model; ---*--- predicted by finite model with stringer attachments, Ref. [14].

where 80% of the reduction results from the mismatch of air density, and 20% from the in-plane tension driven by the overpressure. While at low frequencies, below the associated ring frequency, the influence of the overpressure is dominated by the shift of the resonant frequencies due indirectly by the increased in-plane tension resulting from the combined influence of overpressure, finite panel size and stiffeners attached to the panel. These combined influences may increase or decrease sound transmission loss, depending on panel details and frequency range of observation.

Acknowledgements

The authors gratefully acknowledge the constructive technique support by Kent Lindgren and Danilo Prelevic, useful discussion with Dr. Andrew Peplow in MWL, and the financial support by EU project, Friendly Aircraft Cabin Environment (FACE).

References

[1] P.W. Smith, Sound transmission through thin cylindrical shell, *Journal of the Acoustical Society of America* 29 (1957) 721–729.
[2] L.R. Koval, On sound transmission into a thin cylindrical shell under "flight conditions", *Journal of Sound and Vibration* 48 (1976) 265–275.
[3] L.R. Koval, Effect of air flow, panel curvature, and internal pressurization on field-incidence transmission loss, *Journal of the Acoustical Society of America* 59 (1976) 1379–1385.
[4] L.R. Koval, Effects of cavity resonances on sound transmission into a thin cylindrical shell, *Journal of Sound and Vibration* 59 (1978) 23–33.
[5] L.R. Koval, On sound transmission into an orthotropic shell, *Journal of the Sound and Vibration* 63 (1979) 51–59.
[6] L.R. Koval, Effects of longitudinal stringers on sound transmission into a thin cylindrical shell, *Journal of Aircraft* 15 (1978) 816–821.
[7] L.R. Koval, On sound transmission into a stiffened cylindrical shell with rings and stringers treated as discrete elements, *Journal of Sound and Vibration* 71 (1980) 511–521.
[8] L.R. Koval, Sound transmission into a laminated composite cylindrical shell, *Journal of Sound and Vibration* 71 (1980) 523–530.
[9] A. Blaise, C. Lesueur, M. Gotteland, M. Barbe, On sound transmission into an orthotropic infinite shell: comparison with Koval's results and understanding of phenomena, *Journal of Sound and Vibration* 159 (1991) 233–243.
[10] B. Liu, L. Feng, Sound transmission through a double-walled cylindrical shell, *Proceeding of the 10th International Congress on Sound and Vibration*, KTH, Stockholm, Sweden, July 2003, pp. 4617–4624.
[11] C.L. Dym, Effects of prestress on acoustic behavior of panels, *Journal of the Acoustical Society of America* 55 (1974) 1018–1021.
[12] C.L. Dym, Comments on effects of prestress on acoustic behavior of panels, *Journal of the Acoustical Society of America* 57 (1975) 1543–1544.
[13] ISO 15186-1:2000, Acoustics—measurement of sound insulation in buildings and of building elements using sound intensity—part 1: laboratory measurements.
[14] B. Liu, L. Feng, A.C. Nilsson, Sound transmission through curved aircraft panels with stringers and ring frames, *Journal of Sound and Vibration* 300 (2007) 949–973.
[15] B. Liu, Influence of baffle size and curvature on sound radiated by vibrating panels, *Proceeding of the 11th International Congress on Sound and Vibration*, St.-Petersburg, Russia, July 2004, pp. 1871–1878.